

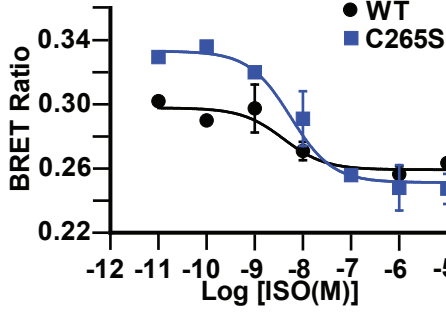


**Supplemental Figure 1. Identification and validation of SNO-sites in  $\beta_2$ AR, Related to Figure 1.**

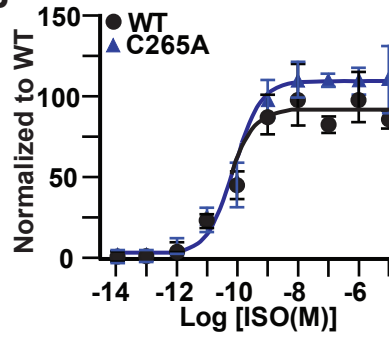
A. SNO- $\beta_2$ AR detected by SNO-RAC of lysates from HEK293 cells stably expressing Flag- $\beta_2$ AR, untreated or treated with ISO (10  $\mu$ M) for the indicated time prior to harvesting cells. The NOS inhibitor L-NMMA was pre-incubated with cells for 2h in indicated lanes. Specificity controls include the absence of ascorbate after free thiol blocking, or photolysis of the nitrosothiol bond during thiol blocking by UV exposure. Total  $\beta_2$ AR control is from Flag immunoblot of lysate. Blot is representative of 3 replicates. B. SNO- $\beta_2$ AR detected by SNO-RAC of lysates from HEK293 cells stably expressing Flag- $\beta_2$ AR, untreated or treated with agonists or partial agonists isoproterenol (ISO), salbutamol (SALB), salmeterol (SALM), pindolol (PIN), procaterol (PROC), fenoterol (FEN), epinephrine (EPI) or isoetharine (iETH) for 10 min at 10  $\mu$ M prior to harvesting cells. Total  $\beta_2$ AR control is from Flag immunoblot of lysate. Blot is representative of 3 replicates. C. Mass spectroscopic identification of  $\beta_2$ AR peptides that contain SNO, following CysNO treatment (100  $\mu$ M, 10 min) of lysates from HEK293 cells stably expressing Flag- $\beta_2$ AR. After SNO-RAC, bead-bound proteins were digested with trypsin, peptides were eluted and SNO-site cysteines were labeled with iodoacetamide prior to mass spectrometry identification. Observed and predicted masses are shown for each identified peptide, and SNO-modified Cys residues are highlighted. D. Mass spectrometry identification of  $\beta_2$ AR peptide containing SNO at Cys265. MS/MS spectra identifying the  $\beta_2$ AR peptide containing Cys265 is shown. E. SNO- $\beta_2$ AR detected by SNO-RAC of lysates from HEK293 cells stably expressing Flag- $\beta_2$ AR WT (W9) or Flag- $\beta_2$ AR 5-Cys mutant (C5A: Cys265/328/341/378/406Ala – all of the intracellular cysteine residues, in two cell clones C5A-1 and C5A-2), untreated or treated with ECNO (100  $\mu$ M, 10 min) prior to harvesting cells. Total  $\beta_2$ AR control is from Flag immunoblot of lysate. Blot shown is representative of 6 replicates. F. SNO- $\beta_2$ AR detected by SNO-RAC of lysates from HEK293 cells stably expressing Flag- $\beta_2$ AR WT (W9) or Flag- $\beta_2$ AR 3-Cys mutant (C3A: Cys265/341/378Ala, the three sites identified by mass spectrometry), untreated or treated with ISO (10  $\mu$ M, 10 min) prior to harvesting cells. Total  $\beta_2$ AR control is from Flag immunoblot of lysate. Blot shown is representative of 7 replicates.  $p < 0.0001$  by one-way ANOVA for treatment; \*  $p < 0.0001$  basal vs ISO by Tukey test. G.  $\beta_2$ AR in HEK cell membranes quantified by [ $^3$ H]-alprenolol binding, from untransfected HEK 293 cells (HEK), wildtype  $\beta_2$ AR -expressing cells (W9), and C265S  $\beta_2$ AR -expressing cells (C265S). Specific binding

was determined using 1 nM [<sup>3</sup>H]-alprenolol in the absence or presence of 1 μM propranolol. No significant difference between W9 and C265S was detected in assays in triplicate using 3 distinct membrane preparations. H. Overexpressed β<sub>2</sub>AR in HEK293 cell membranes detected by western blot using anti-β<sub>2</sub>AR antisera (Santa Cruz H-20, cat # SC-569), from wildtype β<sub>2</sub>AR-expressing cells (W9) and C265S β<sub>2</sub>AR-expressing cells (C265S). Untransfected HEK 293 cells (HEK) were used as a negative control, and GAPDH was detected as a loading control. I. SNO-β<sub>1</sub>-adrenergic receptor (β<sub>1</sub>AR) detected by SNO-RAC of lysates from human heart samples, from normal non-failing heart, ischemic failing heart, and non-ischemic failing heart. Total β<sub>1</sub>AR control is from anti-β<sub>1</sub>AR immunoblot of lysate. Representative blot is shown, of 3 non-failing, 3 ischemic and 3 non-ischemic failing heart samples tested, which are all quantified in the bar graph. \* *p*<0.05 vs non-failing heart by one-way ANOVA with Tukey post-hoc test. J. SNO-Angiotensin II receptor 1 (ATR1) detected by SNO-RAC of lysates from HEK293 cells stably expressing HA-tagged ATR1, without or with angiotensin II peptide (AngII, 10 μm, 10 min). Total ATR1 control is from anti-HA immunoblot of lysate. Blot shown is representative of 3 replicates, which are all quantified in the bar graph. \* *p*<0.05 by t-test.

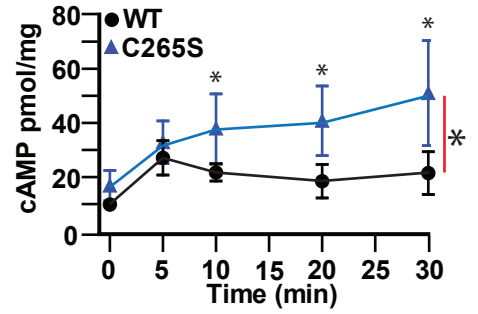
**A**



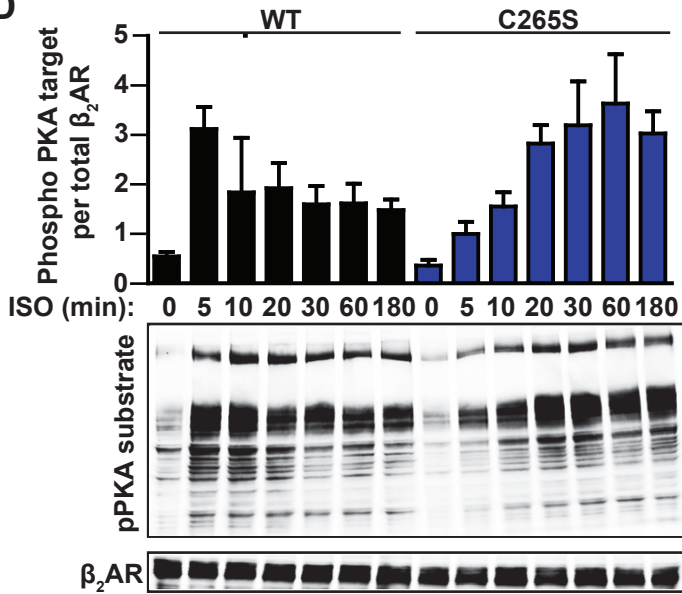
**B**



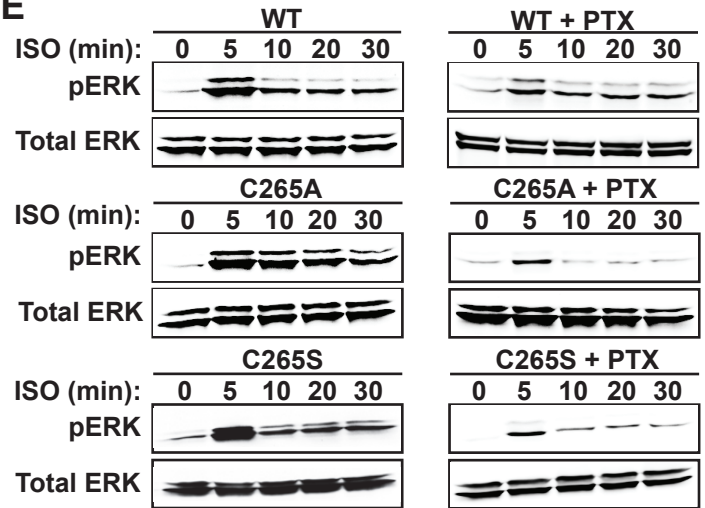
**C**



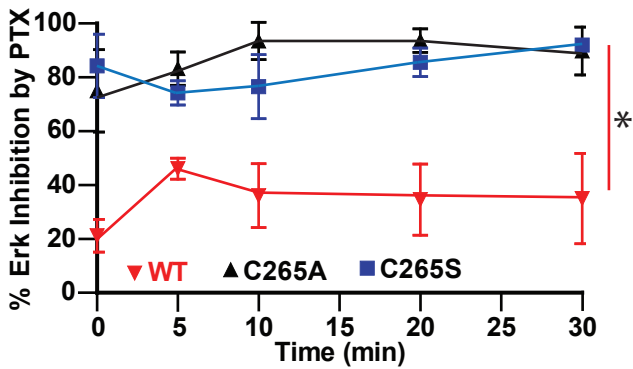
**D**



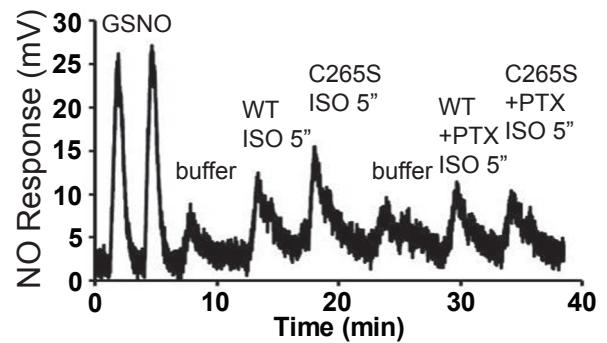
**E**



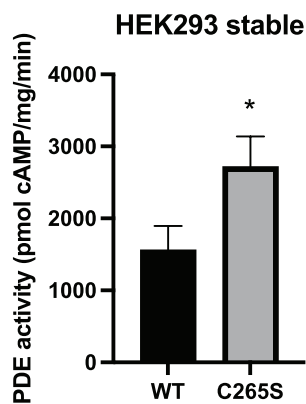
**F**



**G**



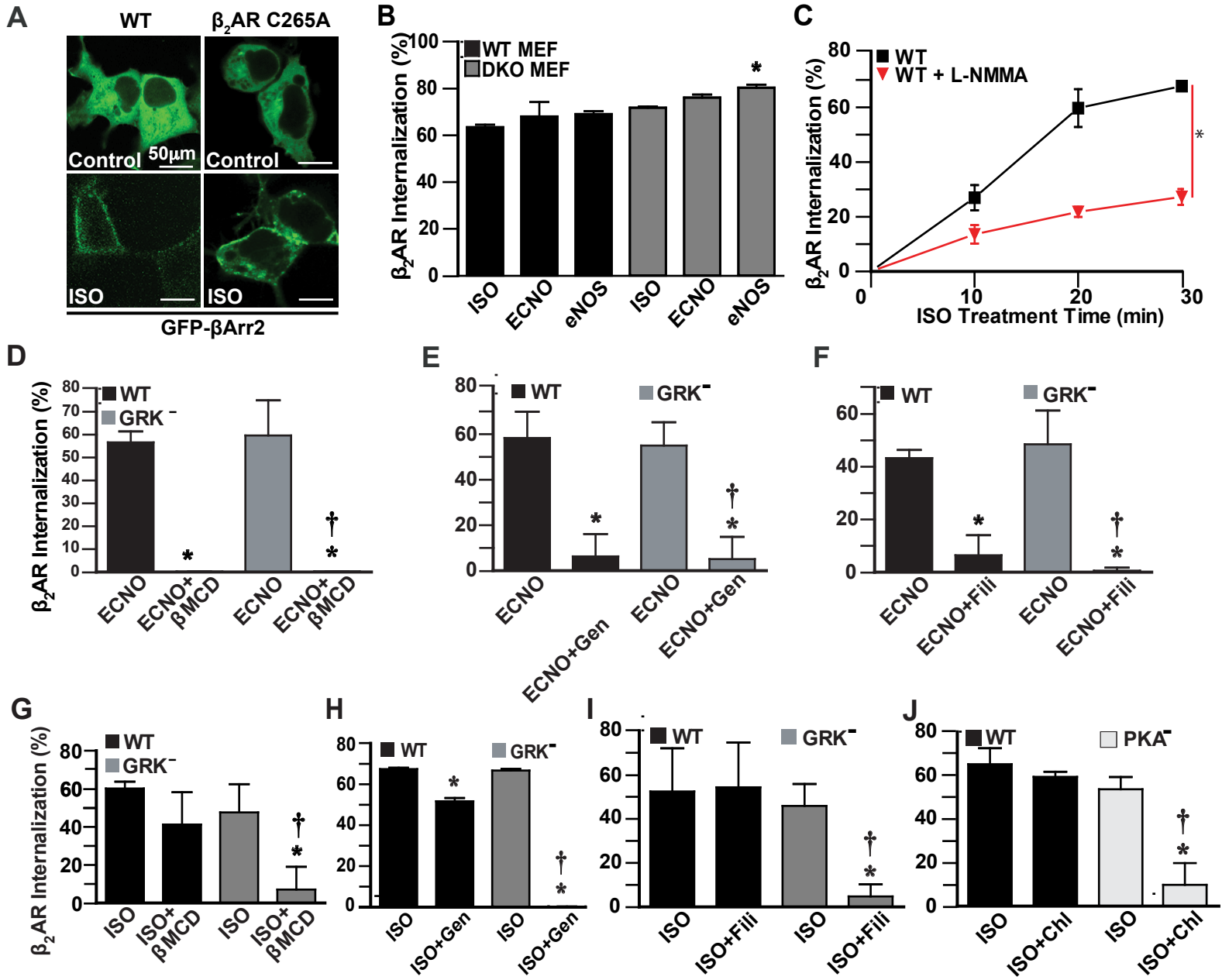
**H**





**Supplemental Figure 2.  $\beta_2$ AR S-nitrosylation at Cys265 does not affect short-term cAMP signaling, Related to Figure 2.** A. Dose response of ISO-stimulated (10 min) cAMP accumulation in HEK293 cells stably expressing Flag- $\beta_2$ AR WT or Flag- $\beta_2$ AR-C265S mutation, measured using the cAMP BRET biosensor CAMYEL. Data are shown as mean $\pm$ SD for 2 assays ( $p$ =ns). B. Dose response of ISO-stimulated (5 min) cAMP accumulation in HEK293 cells stably expressing Flag- $\beta_2$ AR WT or Flag- $\beta_2$ AR -C265A mutation, measured using the GloSensor cAMP assay. Data are shown as mean $\pm$ SD for 3 assays in triplicate ( $p$ =ns). C. Time course of ISO (10  $\mu$ M)-stimulated cAMP accumulation in HEK293 cells stably expressing Flag- $\beta_2$ AR WT or Flag- $\beta_2$ AR-C265S mutation for the indicated times, measured using ELISA assay from cell lysates. Data are shown as mean $\pm$ SD for 6 assays.  $p$ <0.005 by repeated measures ANOVA for genotype, time and time x genotype; \*  $p$ <0.05 for individual time-points by Sidak test. D. Time course of ISO (10  $\mu$ M)-stimulated PKA activity in HEK293 cells stably expressing Flag- $\beta_2$ AR WT or Flag- $\beta_2$ AR-C265S mutation for the indicated times, measured using immunoblotting for pan-PKA phosphorylated target site from cell lysates. Total  $\beta_2$ AR control is from Flag immunoblot of lysate. Image is representative of 4 assays. E. Time course of ISO (10  $\mu$ M)-stimulated Erk activation in HEK293 cells stably expressing Flag- $\beta_2$ AR WT (W9) or Flag- $\beta_2$ AR-C265S or -C265A mutations for the indicated times, measured using immunoblotting for phospho-Thr202/Tyr204-Erk1/2 from cell lysates. Cells were preincubated with 100 ng/ml PTX overnight, or untreated. Total  $\beta_2$ AR control is from Flag immunoblot of lysate. Images are representative of 4 assays. F. Quantification of pErk data (from panel E, and alternately plotted in Fig 1H), shown as % activity that is inhibited by PTX pretreatment. Data are shown as mean $\pm$ SD for 4 assays.  $p$ <0.0001 in a one-way ANOVA among genotypes ( $F(2,9) = 115.3$ ); \*  $p$ <0.0001 for cumulative response (area under curve) for WT vs mutants using Tukey test. G. Raw traces for SNO levels measured by Hg-coupled photolysis/chemiluminescence, in lysates of HEK293 cells expressing WT or C265S  $\beta_2$ AR, pretreated with PTX (100 ng/ml for 16h) or not, and stimulated with ISO (10  $\mu$ M for 5 min), vs GSNO control. Area under curves was quantified by comparison to buffer control and to a standard curve of responses to defined concentrations of GSNO, and are plotted in Fig 2C. H. Basal cAMP phosphodiesterase activity is elevated in HEK293 cells stably expressing  $\beta_2$ AR C265S

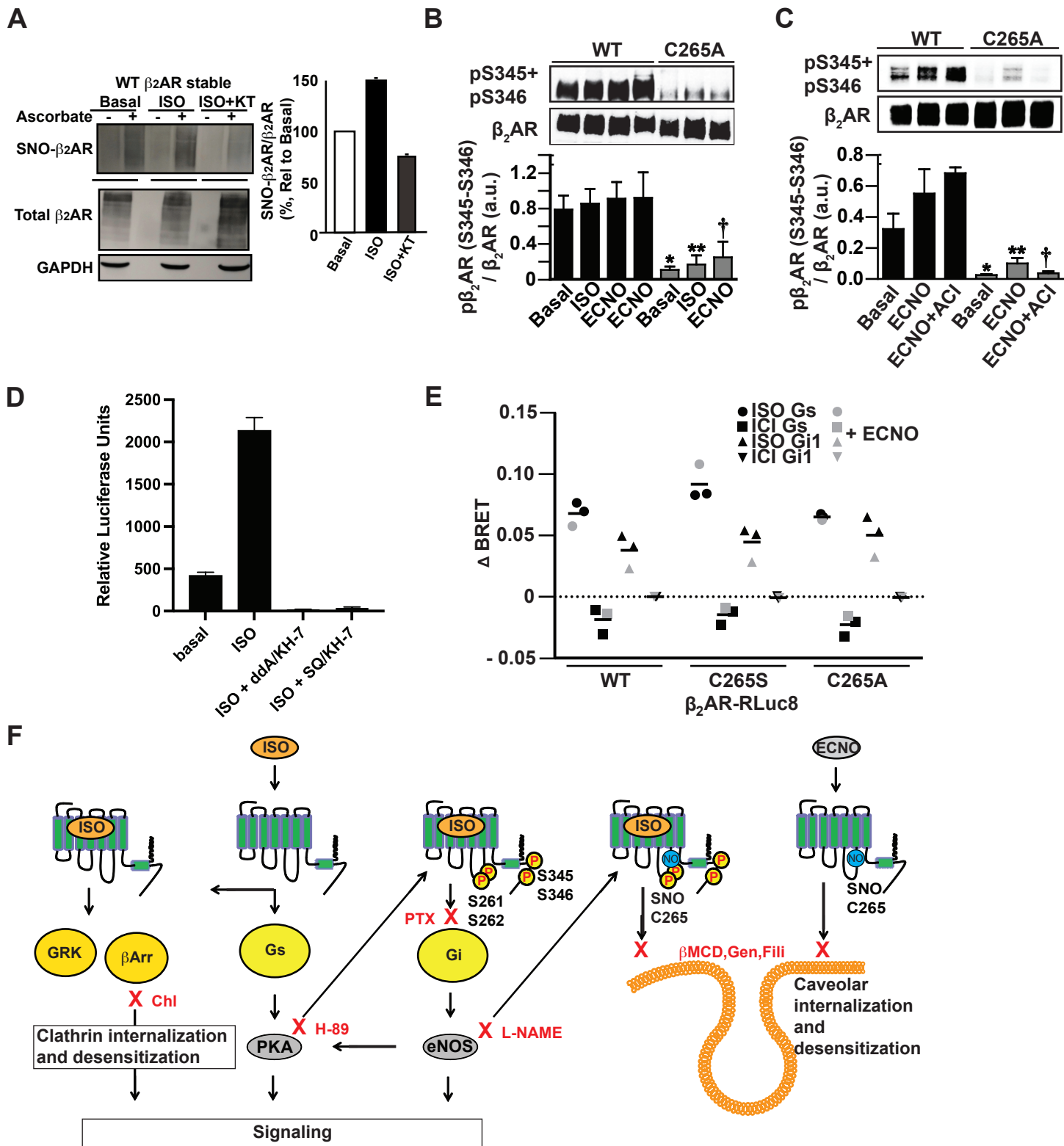
mutant. HEK293 cells stably expressing Flag- $\beta_2$ AR WT (W9) or Flag- $\beta_2$ AR-C265S (C265S) were lysed and assayed for cAMP phosphodiesterase activity. N=3; \*,  $p=0.0004$  by t-test.



**Supplemental Figure 3.  $\beta_2$ AR S-nitrosylation drives agonist-independent receptor internalization through the caveolae pathway, but not the GRK/ $\beta$ -arrestin2/clathrin pathway,**

**Related to Figure 2.** A. Translocation of  $\beta$ -arrestin2-GFP in Flag- $\beta_2$ AR-expressing HEK293 cells stimulated with ISO (10  $\mu$ M) or ECNO (100  $\mu$ M) for 10 min, visualized by confocal microscopy. Data are representative of 15 cells surveyed in 3 experiments. B. Flag- $\beta_2$ AR internalization 10 min after ISO (10  $\mu$ M) or ECNO (100  $\mu$ M), or with eNOS overexpression, in WT MEFs vs  $\beta$ arr1/ $\beta$ arr2 double knockout MEFs (DKO), measured by flow cytometry. Data are shown as mean $\pm$ SD for 3 assays.  $p < 0.0001$  by one-way ANOVA for treatment (F (5, 12) = 14.60); \*  $p < 0.0097$  vs DKO ISO group by Sidak test. C. ISO (10  $\mu$ M) induced time-dependent internalization of cell surface WT Flag- $\beta_2$ AR in stable W9 HEK293 cells is reduced by pretreatment with the eNOS inhibitor L-NMMA (100  $\mu$ M, 16 hours), quantified by flow cytometry. Data are shown as mean $\pm$ SD for 3 assays. \*  $p < 0.0001$  for cumulative response (area under curve) for WT vs drug-treated using two-tail t-test test. D. ECNO-driven (50  $\mu$ M, 20 min) internalization of WT  $\beta_2$ AR or  $\beta_2$ AR deficient in GRK phosphorylation sites (GRK<sup>-</sup>) is inhibited by the caveolae inhibitor  $\beta$ -methyl cyclodextrin ( $\beta$ MCD, 1.5 mM 1h), as measured by flow cytometry. Data are shown as mean $\pm$ SD for 6 assays.  $p < 0.0001$  by one-way ANOVA for treatment (F (3,20) = 104.1); \*  $p < 0.0001$  vs WT ECNO and †  $p < 0.0001$  vs GRK<sup>-</sup> ECNO by Tukey test. E. ECNO-driven (50  $\mu$ M, 20 min) internalization of WT  $\beta_2$ AR and GRK<sup>-</sup>  $\beta_2$ AR is inhibited by pre-incubation with the tyrosine kinase inhibitor genistein (Gen, 200  $\mu$ M for 1h) to inhibit the caveolae pathway, as measured by flow cytometry. Data are shown as mean $\pm$ SD for 6 assays.  $p < 0.0001$  by one-way ANOVA for treatment (F (3,20) = 48.23); \*  $p < 0.0001$  vs WT ECNO and †  $p < 0.0001$  vs GRK<sup>-</sup> ECNO by Tukey test. F. ECNO-driven (50  $\mu$ M, 20 min) internalization of WT  $\beta_2$ AR and GRK<sup>-</sup>  $\beta_2$ AR is inhibited preincubation by the cholesterol-sequestering caveolae inhibitor filipin III (Fili, 800 ng/mL for 1h) used to inhibit the caveolae pathway, as measured by flow cytometry. Data are shown as mean $\pm$ SD for 6 assays.  $p < 0.0001$  by one-way ANOVA for treatment (F (3,20) = 62.82); \*  $p < 0.0001$  vs WT ECNO and †  $p < 0.001$  vs GRK<sup>-</sup> ECNO by Tukey test. G. ISO-driven (10  $\mu$ M, 20 min) internalization of WT  $\beta_2$ AR is not inhibited by the caveolae inhibitor  $\beta$ -methyl cyclodextrin ( $\beta$ MCD, 1.5 mM 1h), while internalization of GRK<sup>-</sup> mutant  $\beta_2$ AR is markedly inhibited, as measured by flow cytometry. Data are shown as mean $\pm$ SD for 6 assays.  $p < 0.0001$  by one-way ANOVA for treatment (F (3,20) = 52.05); \*  $p < 0.0001$  vs WT

ECNO and †  $p < 0.0001$  vs GRK<sup>-</sup> ECNO by Tukey test. H. ISO-driven (10  $\mu$ M, 20 min) internalization of WT  $\beta_2$ AR is partially inhibited by the caveolae inhibitor genistein (Gen, 200  $\mu$ M for 1h), while internalization of GRK<sup>-</sup>  $\beta_2$ AR is markedly inhibited, as measured by flow cytometry. Data are shown as mean $\pm$ SD for 3 assays.  $p < 0.0001$  by one-way ANOVA for treatment (F (3,8) = 3214); \*  $p < 0.0001$  vs WT ISO and †  $p < 0.0001$  vs GRK<sup>-</sup> ISO by Tukey test. I. ISO-driven (10  $\mu$ M, 20 min) internalization of WT  $\beta_2$ AR is not inhibited by the caveolae inhibitor filipin III (Fili, 800 ng/mL for 1h), while internalization of GRK<sup>-</sup>  $\beta_2$ AR is markedly inhibited, as measured by flow cytometry. Data are shown as mean $\pm$ SD for 6 assays.  $p < 0.0001$  by one-way ANOVA for treatment (F (3,20) = 14.09); \*  $p < 0.0001$  vs WT ISO and †  $p < 0.001$  vs GRK<sup>-</sup> ISO by Tukey test. J. ISO-driven (10  $\mu$ M, 20 min) internalization of WT  $\beta_2$ AR is not inhibited by the clathrin inhibitor chlorpromazine (Chl, 10  $\mu$ M 1h), while internalization of  $\beta_2$ AR deficient in PKA phosphorylation sites (PKA<sup>-</sup>) is markedly inhibited, as measured by flow cytometry. Data are shown as mean $\pm$ SD for 3 assays in triplicate.  $p < 0.0001$  by one-way ANOVA for treatment (F (3,32) = 75.29); \*  $p < 0.0001$  vs WT ISO and †  $p < 0.0001$  vs PKA<sup>-</sup> ISO by Tukey test.



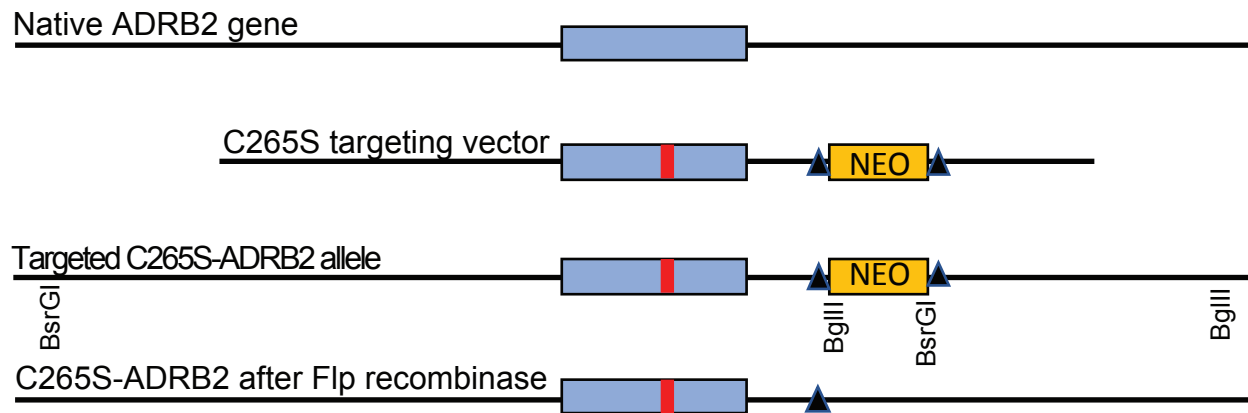
**Supplemental Figure 4. Co-regulation of  $\beta_2$ AR by S-nitrosylation and PKA phosphorylation, and receptor-G protein coupling, Related to Figure 3.**

A. SNO- $\beta_2$ AR detected by SNO-RAC of membrane lysates from HEK293 cells stably expressing Flag- $\beta_2$ AR WT (W9), preincubated in the absence or presence of the PKA inhibitor KT-5720 (10  $\mu$ M, 30 min), and treated with ECNO (100  $\mu$ M, 10 min). Total  $\beta_2$ AR control is from Flag immunoblot of membrane lysate. Blot shown on left is representative of 2 replicates, which are quantified in the graph on the right. B. PKA phosphorylation of Flag- $\beta_2$ AR WT and Flag- $\beta_2$ AR C265A mutant in stable HEK293 cells, stimulated with ISO (10  $\mu$ M, 10 min) or ECNO (100  $\mu$ M, 10 min), detected by immunoblotting of cell lysates using anti-phospho-Ser345/Ser346- $\beta_2$ AR antiserum. Blots are representative of 3 replicates that were quantified by densitometry and plotted as mean $\pm$ SD.  $p < 0.0001$  by one-way ANOVA for treatment  $F(6, 14) = 13.86$ ; \*  $p < 0.0043$  comparing basal, \*\*  $p < 0.0040$  comparing ISO, †  $p < 0.0054$  comparing ECNO by Tukey test. C. Protein kinase A-mediated phosphorylation of the Flag- $\beta_2$ AR WT and Flag- $\beta_2$ AR C265A mutant in stable HEK293 cells, pretreated with adenylyl cyclase inhibitor cocktail for 1h, stimulated with ECNO (100  $\mu$ M, 10 min), detected by immunoblotting of cell lysates using anti phospho-Ser345/Ser346- $\beta_2$ AR antiserum. Blot shown is representative of 3 replicates that were quantified by densitometry and plotted as mean $\pm$ SD.  $p < 0.0001$  by one-way ANOVA for treatment ( $F(5, 12) = 37.79$ ); \*  $p = 0.0063$  vs basal, \*\*  $p = 0.0002$  vs WT ECNO and †  $p < 0.001$  vs ECNO+ACI by Tukey test. D. Isoproterenol-stimulated cAMP accumulation in Flag- $\beta_2$ AR WT HEK293 cells is ablated in the presence of adenylyl cyclase inhibitors. W9 cells were transfected with pGlo-20F GloSensor plasmid, and preincubated with DMSO vehicle or with adenylyl cyclase inhibitors 2',5' dideoxyadenosine 3'-triphosphate 10  $\mu$ M + KH-7 50  $\mu$ M (ddA/KH7) or SQ-22536 10  $\mu$ M + KH-7 50  $\mu$ M (SQ/KH7) for 1h. cAMP accumulation was assessed after stimulation with 10  $\mu$ M isoproterenol (ISO) for 10 min on a Promega GloMax instrument. Data from 3 assays are plotted mean $\pm$ SD. †,  $p < 0.0001$  vs. ISO alone by one-way ANOVA and Tukey test. E. Coupling of RLuc8-fused  $\beta_2$ AR WT or C265S/C265A mutants to overexpressed  $G_s$  or  $G_{i1}$  in HEK293 cells, measured by BRET to split Venus-tagged (Venus 156-239)- $G\beta_1$  and (Venus 1-155)- $G\gamma_2$ . Data for 3 experiments is shown, with mean value indicated as a line. F. Model for  $\beta_2$ AR activation of eNOS leading to SNO- and PKA-mediated internalization of the  $\beta_2$ AR. In the traditional model of ISO-stimulated  $\beta_2$ AR action, the active receptor couples to  $G_s$  to activate PKA,

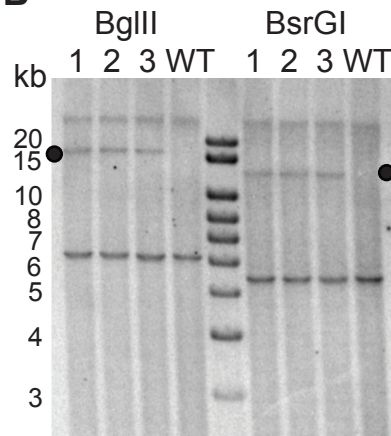
and is phosphorylated by GRKs leading to  $\beta$ -arrestin-mediated signaling and receptor internalization through clathrin coated pits (left side). PKA can phosphorylate the  $\beta_2$ AR at Ser261/262 and Ser345/246 (center), promoting activation of  $G_i$  and reducing coupling to  $G_s$ . Among the  $G_i$ -activated effectors is eNOS, which produces NO. In our study, we find that  $\beta_2$ AR activation (or the NO donor ECNO alone, far right) promotes S-nitrosylation of  $\beta_2$ AR at Cys265 and trafficking of the receptor in caveolae, even in the absence of agonist. This trafficking is inhibited by the caveolae inhibitors  $\beta$ -methyl-D-cyclodextrin ( $\beta$ MCD), genistein (Gen) and Filipin III (Fili), the eNOS inhibitor L-NAME (or L-NMMA), the  $G_i$  inhibitor pertussis toxin (PTX) and the PKA inhibitor H-89, as well as by mutation of  $\beta_2$ AR C265S, Ser261,262,345,346Ala (PKA<sup>-</sup>), but not by the clathrin inhibitor chlorpromazine (Chl) or the GRK<sup>-</sup>  $\beta_2$ AR mutant.



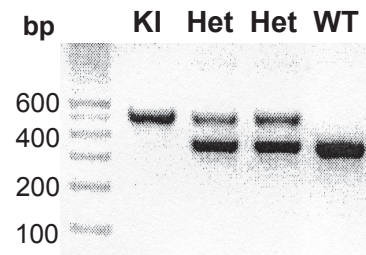
**A**



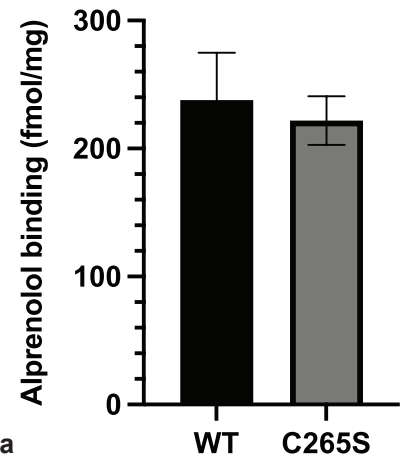
**B**



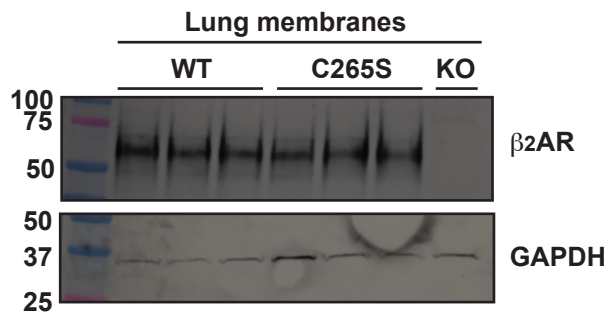
**C**



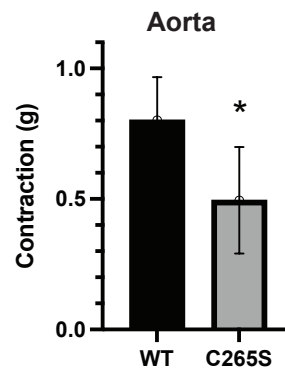
**D**



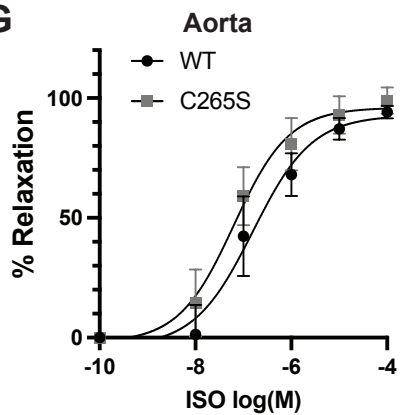
**E**



**F**

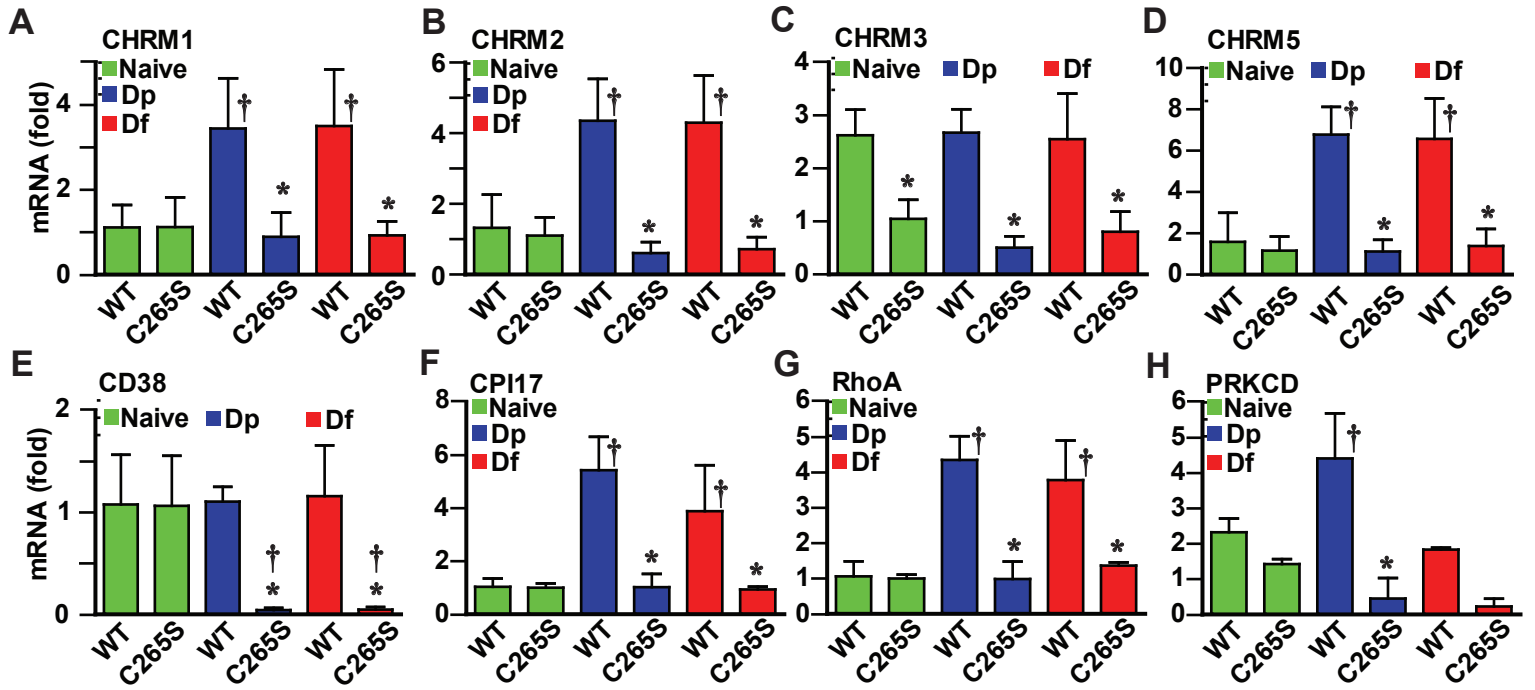


**G**

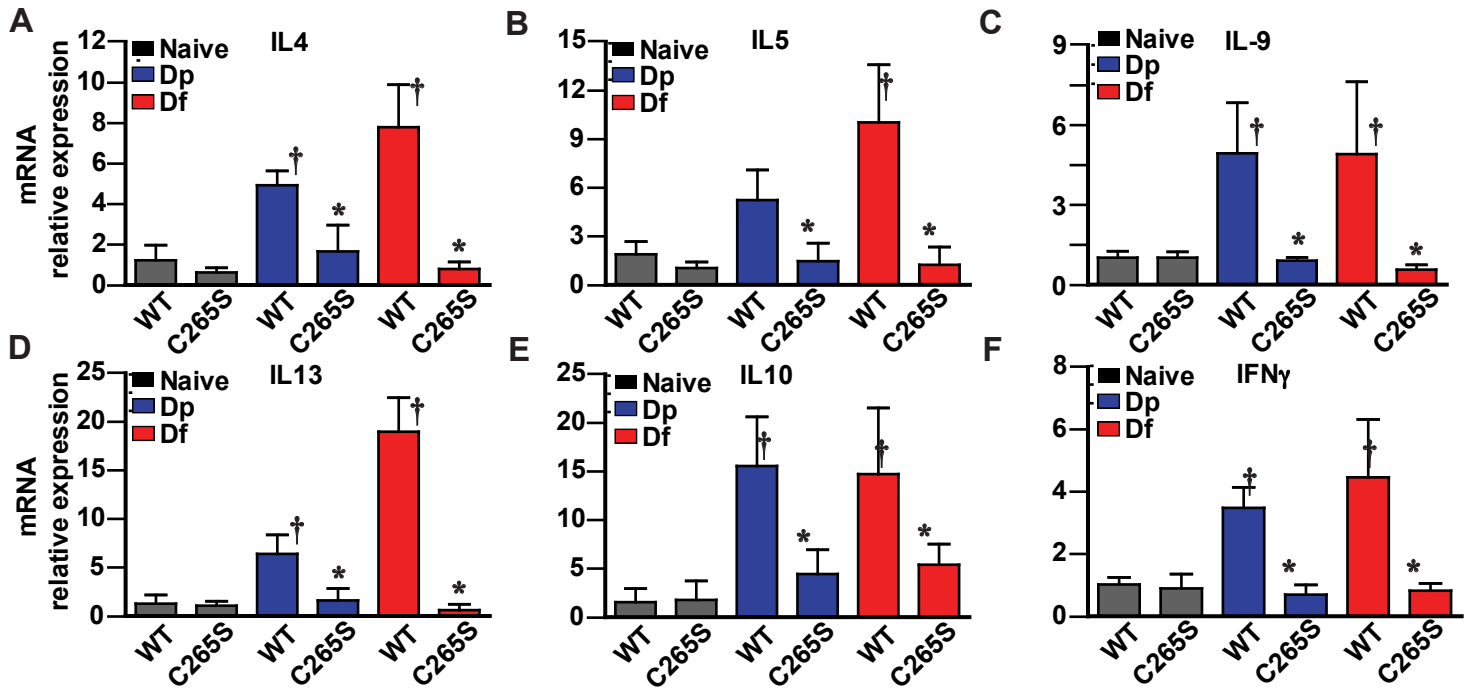


**Supplemental Figure 5. Generation of  $\beta_2$ AR C265S knock-in mouse model, Related to STAR Methods (“Animals”) and Figure 4.**

A. Strategy for generating  $\beta_2$ AR C265S knock-in mice. Mice were generated by homologous recombination in C57BL/6 ES cells using a targeting vector bearing the ADRB2 C265S gene (mutated TGC to TCC, red line) with a loxP/Frt-flanked NEO cassette followed by injection of targeted ES cells into mouse embryos, and the NEO cassette was removed in vivo by breeding heterozygote mice with Flp deleter mice to recombine at Frt sites (black triangles) and selecting for loss of NEO selection marker. B. Validation of integration and point mutation. Proper targeted integration was confirmed by Southern blot. Genomic DNA from targeted ES cell clones (1-3) and a WT clone was digested with BglII or BsrGI and probed with NEO to identify 16kb and 12kb bands, respectively (marked with black circles), indicating proper targeting in ES cell clones for embryo injection. In addition, DNA product bands from PCR amplification across the mutation site in genomic DNA from selected ES clones was sequenced to verify the C265S mutation. C. Genotyping of  $\beta_2$ AR C265S knock-in mice. PCR amplification across the residual loxP/FRT site yields a larger product band in the C265S knock-in (552 bp) compared to WT (372 bp). A representative genotyping reaction is shown identifying homozygous knock-in (KI), heterozygote (Het) and wildtype (WT) pups. D.  $\beta_2$ AR in mouse lung membranes quantified by [ $^3$ H]-alprenolol binding, from wildtype mice (WT), and  $\beta_2$ AR C265S knock-in mice (C265S). Specific binding was determined using 1 nM [ $^3$ H]-alprenolol in the absence or presence of 1  $\mu$ M propranolol. No significant difference between WT and C265S was detected in assays in triplicate assays using lung membrane preparations from 3 distinct mice. E. Native  $\beta_2$ AR in lung membranes detected by western blot using anti- $\beta_2$ AR antisera (Santa Cruz H-20, cat # SC-569), from 3 wildtype mice (WT) and 3  $\beta_2$ AR C265S knock-in mice (C265S). A single  $\beta_2$ AR knockout mouse (KO) was used as a negative control, and GAPDH was detected as a loading control. F. Phenylephrine-stimulated contraction of wildtype versus C265S aorta ex vivo. Tension generated by aortic rings differed between genotypes. N=8 each; \*, p<0.005 by t-test. G. ISO dose-response for relaxation of aorta ex vivo. Wildtype and C265S mouse aortas pretensioned with phenylephrine in (F) were tested for relaxation to increasing doses of ISO, as indicated. No significant difference, p=0.134 by 2-way ANOVA. n=7 WT and n=8 C265S aortas tested.



**Supplemental Figure 6.  $\beta_2AR$  C265S mouse lung lacks muscarinic compensation in allergic asthma model, Related to Figure 5.** A.-H. Quantitative realtime PCR measurement of expression of muscarinic signaling and contractile machinery genes in RNA isolated from whole lung from WT and  $\beta_2AR$  C265S mice treated with the indicated house dust mite allergens (naïve, D.p., D.f.). (A) Chrm1, (B) Chrm2, (C) Chrm3, (D) Chrm5, (E) Cd38, (F) Cpi17, (G) RhoA, (H) Prkcd. Data is shown as mean $\pm$ SD from samples from 3-5 mice.  $p < 0.05$  for all panels B-I by one-way ANOVA; \*  $p < 0.05$  vs corresponding WT treatment control, or †  $p < 0.05$  from corresponding naïve control, by Tukey test.



**Supplemental Figure 7.  $\beta_2AR$  C265S mice fail to induce cytokine expression in allergic asthma model, Related to Figure 6.** A.-F. Quantitative real time PCR measurement of expression of asthma-associated and Th2 cytokine genes in RNA isolated from whole lung from WT and  $\beta_2AR$  C265S mice treated with the indicated house dust mite allergens (naïve, D.p., D.f.). (A) Il4, (B) Il5, (C) Il9, (D) Il13, (E) Il10, (F) Ifng. Data is shown as mean $\pm$ SD from samples from 3-7 mice.  $p < 0.05$  for all panels A-F by one-way ANOVA; \*  $p < 0.05$  vs corresponding WT treatment control, or †  $p < 0.05$  from corresponding naïve control, by Tukey test.

**Supplemental Table I. *Oligonucleotide Primers used for mutagenesis and qPCR, Related to STAR Methods (“Plasmids and Mutagenesis” and “RNA isolation and Realtime reverse transcription-PCR”) and Figures 5 and 6.***

Oligonucleotides		
ADRB2 C265S	5'-TCT TCC AAG TTC TCC TTG AAG GAG CAC	5'-GTG CTC CTT CAA GGA GAA CTT GGA AGA
ADRB2 C265A	5'-TCT TCC AAG TTC GCC TTG AAG GAG CAC	5'-GTG CTC CTT CAA GGC GAA CTT GGA AGA
ADRB2 C327A	5'-CCC CTT ATC TAC GCC CGC AGC CCA GAT	5'-ATC TGG GCT GCG GGC GTA GAT AAG GGG
ADRB2 C341S	5'-CAG GAG CTT CTG TCC CTG CGC AGG TCT	5'-AGA CCT GCG CAG GGA CAG AAG CTC CTG
ABRB2 C341A	5'-CAG GAG CTT CTG GCC CTG CGC AAG TCT	5'-AGA CTT GCG CAG GGC CAG AAG CTC CTG
ADRB2 C378A	5'-AAT AAA CG CTG GCT GAA GAC CTC CCA	5'-TGG GAG GTC TTC AGC CAG CAG TTT ATT
ABRB2 C406A	5'-CAA GGG AGG AAT GCT AGT ACA AAT GAC	5'-GTC ATT TGT ACT AGC ATT CCT CCC TTG
Adrb2 qPCR	5'-TGCTATCACATCGCCCTTC	5'-ACCACTCGGGCCTTATTCTT
Chrm1 qPCR	5'-GGCTGGGCAGTGCTACAT	5'-ATGGCTGTGCCAAAAGTGAT
Chrm2 qPCR	5'-ACTAGTGGGATCGTCAGGTCA	5'-ATTTTGGGGCTACAATGTT
Chrm3 qPCR	5'-TGATGAAGAGGATATTGGCTCA	5'-GGCAGCTTGAGTACAATGGAA
Chrm5 qPCR	5'-GGCCCAGAGAGTACGGAAC	5'-GTTGTTGAGGTGCTTCTACGG
Cd38 qPCR	5'-AAGATGTTCCACCCTGGAGGA	5'-ACTCCAATGTGGGCAAGAGA
Cpi17 qPCR	5'-GAGAAGTGGATCGACGGATG	5'-TCCGGCATGTCTGACTCC
RhoA qPCR	5'-GAATGACGAGCACACGAGAC	5'-TCCTGTTTGCCATATCTCTGC
Prkcd qPCR	5'-CAAGAAGAACAACGGCAAGG	5'-TGCACACACATCAGCACCT
IL1b qPCR	5'-AGTTGACGGACCCCAAAG	5'-AGCTGGATGCTCTCATCAGG
IL4 qPCR	5'-CATCGGCATTTTGAACGAG	5'-CGAGCTCACTCTCTGTGGTG
IL5 qPCR	5'-ACATTGACCGCCAAAAGAG	5'-ATCCAGGAACTGCCTCGTC
IL9 qPCR	5'-GCCTCTGTTTTGCTCTTCAGTT	5'-GCATTTTGACGGTGGATCAT
IL10 qPCR	5'-ACTGCACCCACTTCCCAGT	5'-TGTCCAGCTGGTCCTTTGTT
IL12a qPCR	5'-TCAGAATCACACCATCAGCA	5'-CGCCATTATGATTCAGAGACTG
IL12b qPCR	5'-TTGCTGGTGTCTCCACTCAT	5'-GGGAGTCCAGTCCACCTCTAC
IL13 qPCR	5'-CCTCTGACCCTTAAGGAGCTTAT	5'-CGTTGCACAGGGGAGTCT
Ifng qPCR	5'-ATCTGGAGGAACTGGCAAAA	5'-TTCAAGACTTCAAAGAGTCTGA GGTA
TNFa qPCR	5'-TCTTCTCATTCTGCTTGTGG	5'-GGTCTGGGCCATAGAAGTGA
Actb qPCR	5'-GGCTGTATTCCCCTCCATCG	5'-CCAGTTGGTAACAATGCCATGT

Plcb3 qPCR	5'-AAAAAGCCCACCACTGATGA	5'-ACATCTCCTCCGTGGCATT
Pkca qPCR	5'-ACCGCCGACTGTCTGTAGAA	5'-CCCATGAAGTCATTCCGAGT
RhoK qPCR	5'-AACGGAGGTGACGTGAGGTA	5'-CGGTAGACAATGCGTCTCTG